

Syn–Anti Isomerism in a Mixed-Ligand Oxorhenium Complex, ReO[SN(R)S][S]

M. S. Papadopoulos, I. C. Pirmettis, M. Pelecanou, C. P. Raptopoulou, A. Terzis, C. I. Stassinopoulou, and E. Chiotellis*

Institutes of Radioisotopes–Radiodiagnostic Products, Biology, and Materials Science, NCSR “Demokritos”, POB 60228, 15310, Aghia Paraskevi, Athens, Greece

Received April 17, 1996[⊗]

The simultaneous action of the tridentate ligand $(\text{C}_2\text{H}_5)_2\text{NCH}_2\text{CH}_2\text{N}(\text{CH}_2\text{CH}_2\text{SH})_2$ and the monodentate coligand $\text{HSC}_6\text{H}_4\text{OCH}_3$ on a suitable ReO^{3+} precursor results in a mixture of *syn*- and *anti*-oxorhenium complexes, $\text{ReO}[(\text{C}_2\text{H}_5)_2\text{NCH}_2\text{CH}_2\text{N}(\text{CH}_2\text{CH}_2\text{S})_2][\text{SC}_6\text{H}_4\text{OCH}_3]$, in a ratio of 25/1. The complexes are prepared by a ligand exchange reaction using $\text{ReO}(\text{eg})_2$ (eg = ethylene glycol), $\text{ReOCl}_3(\text{PPh}_3)_2$, or $\text{Re}(\text{V})$ –citrate as precursor. Both complexes have been characterized by elemental analysis, FT-IR, UV–vis, X-ray crystallography, and NMR spectroscopy. The *syn* isomer $\text{C}_{17}\text{H}_{29}\text{N}_2\text{O}_2\text{S}_3\text{Re}$ crystallizes in the monoclinic space group $P2_1/n$, $a = 14.109(4)$ Å, $b = 7.518(2)$ Å, $c = 20.900(5)$ Å, $\beta = 103.07(1)^\circ$, $V = 2159.4(9)$ Å³, $Z = 4$. The *anti* isomer $\text{C}_{17}\text{H}_{29}\text{N}_2\text{O}_2\text{S}_3\text{Re}$ crystallizes in $P2_1/n$, $a = 9.3850(7)$ Å, $b = 27.979(2)$ Å, $c = 8.3648(6)$ Å, $\beta = 99.86(1)^\circ$, $V = 2163.9(3)$ Å³, $Z = 4$. Complete NMR studies show that the orientation of the N substituent chain with respect to the $\text{Re}=\text{O}$ core greatly influences the observed chemical shifts. Complexes were also prepared at the tracer (^{186}Re) level by using ^{186}Re –citrate as precursor. Corroboration of the structure at tracer level was achieved by comparative HPLC studies.

Introduction

The coordination chemistry of technetium and rhenium currently is attracting much attention due to the radionuclide-based application in radiopharmaceuticals. $^{99\text{m}}\text{Tc}$ is the radionuclide of choice for diagnostic imaging due to its ideal nuclear properties ($t_{1/2} = 6$ h, $\gamma = 140$ keV) and wide availability. On the other hand, ^{186}Re and ^{188}Re as β -emitters ($E_{\text{max}} = 1.1$ and 2.1 MeV, respectively) are two of the most promising candidates for radiotherapy.¹ The half-life of ^{186}Re is 90.64 h with a γ -line of 137 keV (9.5%), and the half-life of ^{188}Re is 17 h with a γ -line of 155 keV (15%).

Our recent work involves the study of mixed-ligand systems (3+1 combination) as chelating systems for oxotechnetium. We have reported previously the synthesis and characterization of a series of neutral, lipophilic technetium complexes, TcOL1L2 , where L1H_2 is a tridentate ligand (SNS donor atom set) and L2H is a monodentate thiol acting as coligand.² Formation of these complexes is based on the simultaneous action of

equimolar quantities of the tridentate and monodentate coligands on a suitable TcO^{3+} precursor.³ This ligand system has been shown to form complexes of the same structure at the tracer level ($^{99\text{m}}\text{Tc}$). Distribution studies in mice demonstrated significant uptake and retention of these $^{99\text{m}}\text{Tc}$ complexes in the brain.⁴

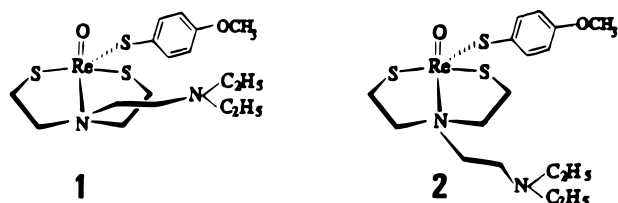
Rhenium, as technetium's third-row congener, exhibits many of the chemical properties of technetium.⁵ Because of the analogy in the chemistry of rhenium and technetium and the recent availability of radionuclides of rhenium, the use of this ligand combination [3+1, (SNS)(S) donor atom set] may be further expanded for the preparation of rhenium complexes for therapeutic applications. We report here the synthesis, structure, and chemical properties of a representative complex of the general formula ReOL1L2 , where $\text{L1H}_2 = (\text{C}_2\text{H}_5)_2\text{NCH}_2\text{CH}_2\text{N}(\text{CH}_2\text{CH}_2\text{SH})_2$ and $\text{L2H} = \text{HSC}_6\text{H}_4\text{OCH}_3$. Since upon complexation the N substituent of the tridentate ligand can assume the *syn* or *anti* configuration with respect to the ReO^{3+} core, two diastereomeric complexes theoretically are possible.⁶ Indeed, we have successfully isolated the two isomers: *syn* (complex **1**) with the side chain on nitrogen directed toward the $\text{Re}=\text{O}$ core and *anti* (complex **2**) with the side chain directed away from the $\text{Re}=\text{O}$ core (Chart 1). Both complexes were characterized by elemental analysis and spectroscopic methods.

* Address correspondence to Efstratios Chiotellis, Ph.D., Institute of Radioisotopes–Radiodiagnostic Products, 15310 Ag. Paraskevi, Athens, Greece. Telephone +301 6513793. Fax: +301 6543526.

[⊗] Abstract published in *Advance ACS Abstracts*, October 1, 1996.

- (1) (a) Volkert, W.; Ketring, A. *J. Nucl. Med.* **1991**, *32*, 174. (b) Deutsch, E.; Libson, K.; Vanderheyden, J.-L.; Ketring, A. R.; Maxin, H.R. *J. Nucl. Med. Biol.* **1986**, *13*, 465. (c) Fritzeberg, A. R.; Vanderheyden, J.-L.; Rao, T. N.; Kasina, S.; Eshima, D.; Taylor, A. T. *J. Nucl. Med.* **1989**, *30*, 60. (d) DiZio, J. P.; Fiaschi, R.; Davison, A.; Jones, A. G.; Katzenellenbogen, J. A. *Bioconjugate Chem.* **1991**, *2*, 353.
- (2) (a) Mastrostamatis, S. G.; Papadopoulos, M. S.; Pirmettis, I. C.; Paschali, E.; Varvarigou, A. D.; Stassinopoulou, C. I.; Raptopoulou, C. P.; Terzis, A.; Chiotellis, E. *J. Med. Chem.* **1994**, *37*, 3212. (b) Stassinopoulou, C. I.; Pelecanou, M.; Mastrostamatis, S.; Chiotellis, E. *Magn. Reson. Chem.* **1994**, *32*, 532. (c) Spyriounis, D.; Pelecanou, M.; Stassinopoulou, C. I.; Raptopoulou, C. P.; Terzis, A.; Chiotellis, E. *Inorg. Chem.* **1995**, *34*, 1077. (d) Mastrostamatis, S.; Pirmettis, I.; Papadopoulos, M.; Paschali, E.; Raptopoulou, C.; Terzis, A.; Chiotellis, E. In *Technetium and Rhenium in Chemistry and Nuclear Medicine 4*; Nicolini, M., Bandoli, G., Mazzi, U., Eds.; SGE: Padova, 1995; p 409. (e) Papadopoulos, M.; Pirmettis, I.; Raptopoulou, C.; Terzis, A.; Chiotellis, E. In *Technetium and Rhenium in Chemistry and Nuclear Medicine 4*; Nicolini, M., Bandoli, G., Mazzi, U., Eds.; SGE: Padova, 1995; p 223. (f) Pirmettis, I.; Papadopoulos, M.; Mastrostamatis, S.; Raptopoulou, C.; Terzis, A.; Chiotellis, E. *Inorg. Chem.* **1996**, *35*, 1685.
- (3) (a) Pietzsch, H.-J.; Spies, H.; Hoffmann, S.; Stach, J. Lipophilic technetium complexes-V. *Inorg. Chim. Acta* **1989**, *161*, 15. (b) Pietzsch, H.-J.; Spies, H.; Hoffmann, S.; Scheller, D. *Appl. Radiat. Isotop.* **1990**, *41*, 185. (c) Spies, H.; Johannsen, B.; Pietzsch, H.; Noll, B.; Noll, St.; Scheunemann, M.; Fietz, T.; Berger, R.; Brust, P.; Leibnitz, P. *XI International Symposium on Radiopharmaceutical Chemistry*, Vancouver, 1995, 319. (d) Spies, H.; Fietz, T.; Glaser, M.; Pietzsch, H.; Johannsen, B. In *Technetium and Rhenium in Chemistry and Nuclear Medicine 4*; Nicolini, M., Bandoli, G., Mazzi, U., Eds.; SGE: Padova, 1995; p 243.
- (4) (a) Pirmettis, I.; Papadopoulos, M.; Paschali, E.; Varvarigou, A.; Chiotellis, E. *Eur. J. Nucl. Med.* **1994**, *21*, S7. (b) Pirmettis, I.; Papadopoulos, M.; Mastrostamatis, S.; Tsoukalas, Ch.; Chiotellis, E. *J. Nucl. Med.* **1995**, *36*, 145P. (c) Pirmettis, I.; Papadopoulos, M.; Paschali, E.; Varvarigou, A. D.; Chiotellis, E. *J. Nucl. Med.* **1995**, *36*, 145P.
- (5) Deutsch, E.; Libson, K.; Vanderheyden, J.-L. In *Technetium and Rhenium in Chemistry and Nuclear Medicine 3*; Nicolini, M., Bandoli, G., Mazzi, U., Eds.; Raven Press: New York, 1990; p 119.

Chart 1



Complete assignments of ^1H and ^{13}C NMR resonances were made and the crystal structures were determined by X-ray crystallography.

Results and Discussion

Synthesis. Three methods were employed for the synthesis of the complexes based on the ligand exchange reaction using $\text{ReO}(\text{eg})_2$ (eg = ethylene glycol), $\text{ReOCl}_3(\text{PPh}_3)_2$, or $\text{Re}(\text{V})$ -citrate as precursor (see Experimental Section, methods A, B, and C) in the presence of equimolar quantities of LiH_2 and L_2H . $\text{ReO}(\text{eg})_2$ and $\text{Re}(\text{V})$ -citrate were used *in situ* as formed either by ligand exchange reaction of ReOCl_4^- and ethylene glycol or by reduction of ReO_4^- by Sn^{2+} in citric acid. The latter method is commonly used to prepare rhenium radiopharmaceuticals since the starting material of radioactive rhenium is ReO_4^- .

In all three methods, reaction products were extracted in dichloromethane and isolated by fractional recrystallization from $\text{CH}_2\text{Cl}_2/\text{MeOH}$. The major product, in all cases, was the *syn* isomer as demonstrated by crystal structure analysis. HPLC detection (C-18 RP column using 85/15 methanol/water as the mobile phase and a flow rate of 1 mL/min) of the crude reaction mixture from the A and B methods revealed the presence of a small amount of an additional complex. This was successfully isolated from the reaction mixture from method A and was identified as the *anti* isomer by X-ray crystallography. HPLC analysis of the reaction mixture from method C showed the formation of only the *syn* isomer.

The *syn* isomer was retained longer on the C-18 column (Figure 1), and the ratio *syn/anti* isomer as calculated by HPLC integration was 25/1. The results are consistent with those of the corresponding technetium isomers previously prepared with this ligand system.^{2f}

Both complexes gave correct elemental analysis and were characterized by IR, UV-vis, and NMR spectroscopy. They are soluble in acetone, dichloromethane, and chloroform, slightly soluble in methanol or ethanol, and insoluble in ether, pentane, and water. They are stable in the solid state as well as in organic solutions (for a period of months) as shown by HPLC and NMR. Their stability is not affected by the presence of air or moisture.

The infrared spectra of the compounds exhibit strong $\text{Re}=\text{O}$ stretching bands at 946 cm^{-1} for the *syn* and 963 cm^{-1} for the *anti* isomer. These values are consistent with those reported for several other well-characterized monooxo complexes of rhenium.⁷ The $\text{Re}=\text{O}$ stretch in each isomer was approximately 20 cm^{-1} higher than the $\text{Tc}=\text{O}$ stretch in the corresponding oxotechnetium isomers.^{2f} This shift to higher frequencies from

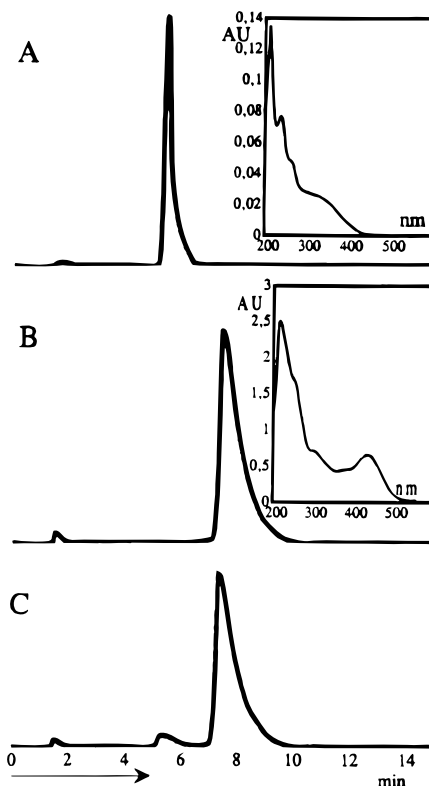


Figure 1. HPLC profiles: (A) UV trace at 254 nm of complex 2 (*anti* isomer); (B) UV trace at 254 nm of complex 1 (*syn* isomer). The UV-vis spectra of both complexes are shown in the insets. (C) γ -trace of the reaction mixture of the ^{186}Re preparation (tracer level).

$\text{Tc}=\text{O}$ to $\text{Re}=\text{O}$ complexes has also been reported for other ligand systems, like BAT and MAMA.^{6f,7a} The electronic absorption spectra of the complexes were determined during HPLC analysis by using the photodiode array detector. The UV-vis spectra of the *syn* isomer are characterized by an intense band at 426 nm, while the *anti* isomer is characterized by an intense band at shorter wavelength (350 nm).

Complexes were prepared at the tracer level by using ^{186}Re -citrate as precursor. The labeling yield was over 80% as calculated by organic solvent extraction of the aqueous reaction mixture. HPLC analysis has shown the formation of two complexes in a ratio 25/1 with the major product having the longest retention time (Figure 1). When mixed samples of complexes prepared at the tracer and carrier levels were injected on the HPLC column, they eluted with identical retention times as witnessed by simultaneous radioactivity (tracer) and UV-vis detection (Figure 1). This indicates that the same chemical species are formed at the carrier and tracer levels.

X-ray Crystallographic Studies. An ORTEP diagram of compound 1 is given in Figure 2, and selected bond distances and angles are given in Table 1. Complex 1 is the *syn* isomer where the coordination geometry around rhenium is distorted trigonal bipyramidal. The basal plane is formed by the sulfur atoms of the tridentate ligand and the oxo group, while the apical positions are occupied by the remaining nitrogen atom of the ligand and the monodentate thiol. The calculated trigonality index, τ , is 0.62.⁸ Rhenium is slightly displaced out of the basal

(6) (a) Epps, L.; Burns, H. D.; Lever, S. Z.; Goldfarb, H. W.; Wagner, H. N. *Appl. Radiat. Isotop.* **1987**, *36*, 661. (b) Kung, H. G.; Guo, Y. Z.; Yu, C. C.; Billings, J.; Subramanyam, V.; Calabrese, J. J. *Med. Chem.* **1989**, *32*, 433. (c) Lever, S. Z.; Baidoo, K. E.; Mahmood, A. *Inorg. Chim. Acta* **1990**, *176*, 183. (d) Rao, T. N.; Adhikesavalu, D.; Camerman, A.; Fritzbeg, A. R. *J. Am. Chem. Soc.* **1990**, *112*, 5798. (e) Francesconi, L. C.; Graczyk, G.; Wehrli, S.; Shaikh, N.; McClinton, D.; Liu, S.; Zubietta, J.; Kung, H. F. *Inorg. Chem.* **1993**, *32*, 3114. (f) O'Neil, J.; Wilson, S.; Katzenellenbogen, J. *Inorg. Chem.* **1994**, *33*, 319.

(7) (a) Mahmood, A.; Baidoo, K. E.; Lever, S. Z. In *Technetium and Rhenium in Chemistry and Nuclear Medicine 3*; Nicolini, M., Bandoli, G., Mazzi, U., Eds.; Raven Press: New York, 1990; p 119 (b) Oisato, F.; Refosco, F.; Mazzi, U.; Bandoli, G.; Nicolini, M. *Inorg. Chim. Acta* **1991**, *189*, 97. (c) Jackson, T.; Kojima M.; Lambrecht, R. M. *Aust. J. Chem.* **1993**, *46*, 1093.

(8) Addison, A. W.; Rao, T. N.; Reedijk, J.; Rijn, J.; Verschoor, G. C. *J. Chem. Soc., Dalton Trans.* **1984**, 1349.

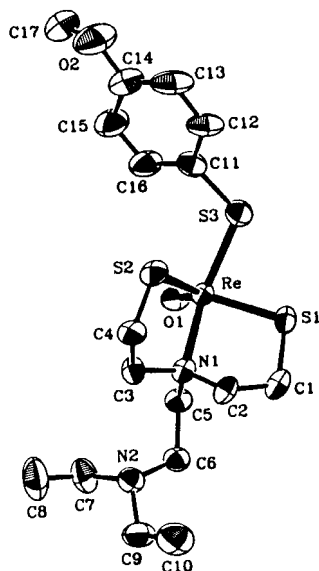


Figure 2. ORTEP diagram of complex **1**, with 50% thermal probability ellipsoids showing the atomic labeling scheme.

Table 1. Selected Bond Distances (Å) and Angles (deg)

	1	2
Re–O1	1.696(5)	1.694(8)
Re–S1	2.279(2)	2.308(3)
Re–S2	2.275(2)	2.297(3)
Re–S3	2.309(2)	2.285(3)
Re–N1	2.218(8)	2.15(1)
O1–Re–S1	117.5(2)	107.9(3)
O1–Re–S2	120.1(2)	107.7(3)
O1–Re–S3	105.2(2)	106.6(4)
O1–Re–N1	95.8(2)	112.2(4)
S1–Re–S2	121.8(1)	143.8(1)
N1–Re–S3	158.8(2)	141.1(3)
S1–Re–N1	83.8(2)	81.2(3)
N1–Re–S2	83.3(2)	79.6(3)
S2–Re–S3	88.45(8)	91.7(1)
S3–Re–S1	84.02(9)	84.3(1)

plane by 0.087 Å toward the monodentate thiol. The two chelating five-membered rings exist in the envelope form where the “flap” atoms are C2 and C3, which are displaced by 0.64 and 0.61 Å from the best mean plane of the remaining atoms (i.e., Re, S1, C1, and N1 and Re, S2, C4, and N1, respectively). The dihedral angles formed by the chelating atoms of the tridentate ligand are 51.4° and 49.4° for S1–C1–C2–N1 and S2–C4–C3–N1, respectively. The bond distances and angles observed in the coordination sphere are in agreement with those found in other oxorhenium complexes with distorted trigonal bipyramidal coordination mode. The bond length Re–S3 [2.309(2) Å] is slightly longer than that found between rhenium and the sulfur atoms of the tridentate ligand [Re–S1 = 2.279(2) Å, Re–S2 = 2.275(2) Å]; the opposite was found for the *anti* isomer. The bond angles between atoms of the basal plane are close to the ideal value of 120° while the angle S3–Re–N1 is 158.8(2)°, indicating the distortion of the trigonal bipyramid.

An ORTEP diagram of compound **2** is shown in Figure 3, and selected bond distances and angles are given in Table 1. As shown in Figure 3, the complex is the *anti* isomer in which the coordination geometry of rhenium is distorted square pyramidal with the oxo group occupying the apical position. The calculated trigonality index, τ , is 0.05. The basal plane of the square pyramid is formed by the SNS donor set of the tridentate ligand and the sulfur atom of the monodentate thiol. Rhenium is displaced 0.72 Å out of the basal plane toward the

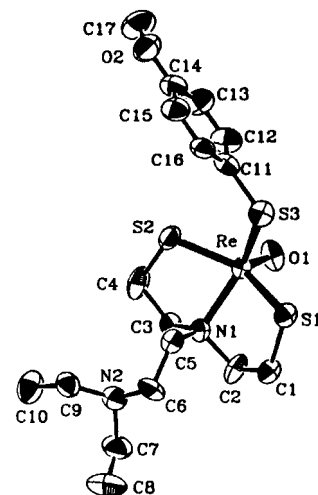


Figure 3. ORTEP diagram of complex **2**, with 50% thermal probability ellipsoids showing the atomic labeling scheme.

oxo group. The two chelating five-membered rings exist in the envelope form where, in both cases, N1 is the “flap” atom and is displaced by 0.86 and 0.89 Å from the best mean plane of the remaining atoms (i.e., Re, S2, C4, and C3 and Re, S1, C1, and C2, respectively). The dihedral angles formed by the chelating agent of the coordinated atoms are 40.7° and 37.3° for S1–C1–C2–N1 and S2–C4–C3–N1, respectively. The bond length Re–S3 is 2.285(3) Å, which is slightly shorter than the corresponding bond distances between rhenium and S1 and S2 belonging to the tridentate ligand [Re–S1 = 2.308 Å, Re–S2 = 2.297(3) Å].

In conclusion, the following remarks should be made: In the case of the *anti* isomer, **2**, where the SNS donor set of the tridentate ligand is coordinated in the basal plane of the distorted square pyramid, the Re–S1 and Re–S2 bond lengths [2.308(3), 2.297(3) Å] are lengthened with respect to Re–S3 [of the monodentate thiol, 2.285(3) Å] and that of Re–N1 is shortened [2.15(1) Å]. In the case of the *syn* isomer, **1**, the opposite is observed; Re–S3 and Re–N1 [2.309(2) and 2.218 Å, respectively] are lengthened as a consequence of occupying the apical positions, while the bond lengths Re–S1 and Re–S2 [2.279(2) and 2.275(2) Å, respectively] in the equatorial plane are shortened. The bond length of the doubly bonded oxo group remains unchanged at ca. 1.69 Å in both cases (i.e., in coordination in the equatorial plane of the distorted trigonal bipyramid or in the apical position of the distorted square pyramid). Differences between the two isomers are also observed in the dihedral angles between the atoms of the chelating skeleton of the tridentate ligand. In the *syn* isomer, **1**, the torsion angles S1–C1–C2–N1 and S2–C4–C3–N1 have the same sign and are greater than those in the *anti* isomer, **2** (51.4°/49.4° and –40.7°/37.3°, respectively).

As already mentioned, the characteristic difference between **1** and **2** is the orientation of the N1 substituent (i.e., C5) toward or away from the oxo group, respectively. This fact is reflected by the dihedral angles around N1, where two differences are seen: in the *syn* isomer, **1**, the torsion angles C2–N1–C3–C4 and C4–C3–N1–C5 are 70.6° and –166.3°, respectively, whereas in the *anti* isomer, **2**, these dihedral angles are –175.2° and 64.0°, respectively. This indicates an interchange in the positions of atoms C2 and C5 in the tetrahedron around N1 in the process of formation of the *syn* or *anti* isomer. This fact is also indicated by the interatomic distances between O1 and C2 and C5 in the two isomers: in the *syn* isomer, **1**, O1···C5 = 2.90 Å and O1···C2 = 4.13 Å, while in the *anti* isomer, **2**, O1···C5 = 4.52 Å, and O1···C2 = 3.61 Å.

Table 2. ^1H Chemical Shifts δ_{H} (ppm) for Complexes **1** and **2** in CDCl_3 at 298 K (25 $^\circ\text{C}$)

	1	2		1	2
H1 <i>endo</i>	3.57 ^c	3.40 ^c	H5 ^b	3.92	2.25 ^c
H1 <i>exo</i>	2.85 ^c	3.40 ^c	H5' ^b	3.92	2.35 ^c
H2 <i>endo</i> ^a	3.43 ^c	3.80 ^c	H6	2.87	2.57
H2 <i>exo</i> ^a	2.78 ^c	4.33 ^c	H7 (H9)	2.58	2.43
H3 <i>endo</i> ^a	3.43 ^c	3.72 ^c	H8 (H10)	1.07	1.00
H3 <i>exo</i> ^a	2.78 ^c	4.30 ^c	H12 (H16)	7.55	7.51
H4 <i>endo</i> ^a	3.57 ^c	3.50 ^c	H13 (H15)	6.91	6.95
H4 <i>exo</i> ^a	2.85 ^c	3.60 ^c	H17	3.83	3.84

^a Resonances appear broad due to chemical exchange between protons H1/H4 and H2/H3. ^b Protons on C5 of the side chain (H5 and H5') are also exchanging due to the decreased mobility of the chelated backbone. In complex **1** they appear as a broadened triplet, while in complex **2** they appear as two separate multiplets. ^c Chemical shifts of overlapping multiplets were defined from the correlation peaks of the 2D experiments.

Table 3. ^{13}C Chemical Shifts δ_{C} (ppm) for Complexes **1** and **2** in CDCl_3 and at 298 K (25 $^\circ\text{C}$)

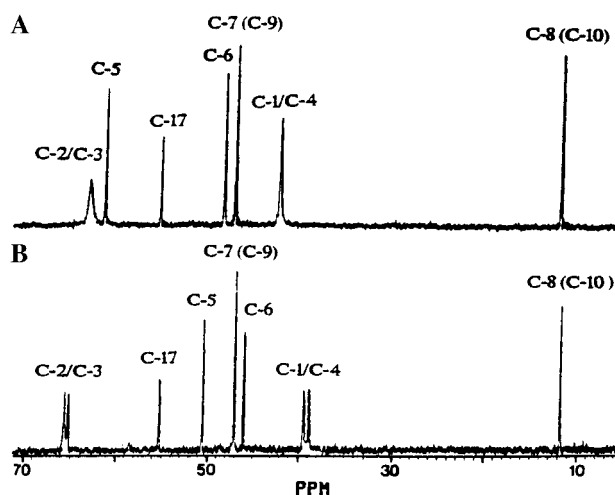
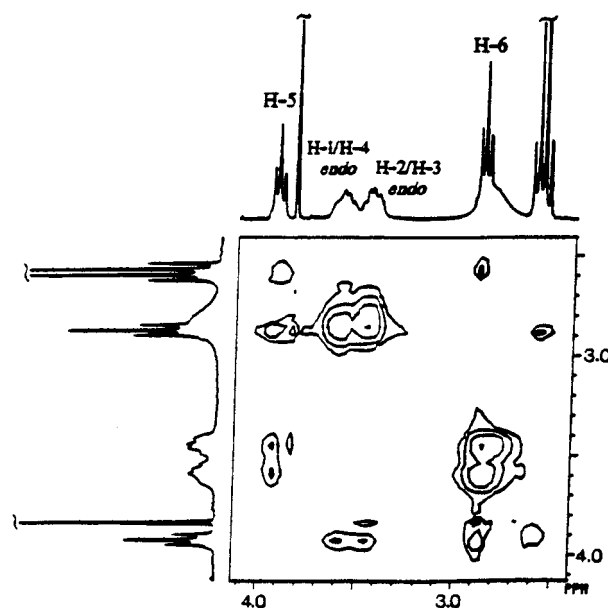
	1	2		1	2
C1 ^a	42.04	39.38	C8 (C10)	11.74	11.79
C2 ^a	62.99	65.60	C11	144.90	140.97
C3 ^a	62.99	65.21	C12 (C16)	134.54	134.60
C4 ^a	42.04	38.84	C13 (C15)	113.56	113.65
C5	61.26	50.53	C14	158.46	158.91
C6	48.21	46.02	C17	55.24	55.25
C7 (C9)	46.99	47.06			

^a Carbons C1/C4 and C3/C4 are in chemical exchange. In complex **1** at 298 K they are above coalescence and appear broad, while in complex **2** they all appear separately (Figure 4).

NMR Studies. The NMR study of *syn* and *anti* stereoisomers of the 3+1 type of complex is of great interest since it provides the opportunity to study the effect of the direction of the free chain on the appearance of the NMR spectra as well as on the fluxional mobility of the coordinated SNS backbone. The ^1H and ^{13}C chemical shifts for complexes **1** and **2** in CDCl_3 at 298 K are given in Tables 2 and 3. Diastereotopic protons on the chelated backbone are differentiated according to their orientation as *endo* (close to oxygen) and *exo* (remote from oxygen).

At room temperature, exchange occurs between the S1–C1–C2–N and S2–C3–C4–N parts of the complexes due to the fluxional mobility of the chelated backbone. Proton resonances appear broad, and the great degree of overlap makes the observation of exchange phenomena in proton spectra very difficult. Carbon spectra are more informative. In the ^{13}C spectrum of the *syn* isomer at 298 K, exchanging carbons C1/C4 and C2/C3 are above the coalescence temperature and appear as one broad resonance (Figure 4A). In the ^{13}C spectrum of the *anti* isomer at the same temperature, exchanging carbons C1/C4 and C2/C3 appear as separate signals, indicating that ring inversion is slow on the NMR time scale (Figure 4B). The relative height of the peaks of the exchanging carbons indicates that the populations of the diastereomeric conformations are equal. Calculation of the ΔG^\ddagger for conformational inversion of the two chelated rings was based on the temperature dependence of the carbon spectra. From the coalescence temperatures of C1/C4 and C2/C3 and the difference in chemical shifts in the absence of exchange, the average ΔG_c^\ddagger was found to be 13.7 \pm 0.1 kcal/mol for complex **1** and 15.9 \pm 0.1 kcal/mol for complex **2**. At 298 K, in CDCl_3 , conformational inversion of the *syn* isomer is 36 times faster than that of the *anti*.

^1H spectra of complexes **1** and **2** were also obtained in the range 25–85 $^\circ\text{C}$ in toluene- d_8 . As the temperature was raised, proton multiplet peaks became sharper, indicating increased

**Figure 4.** ^{13}C spectra (range δ_{C} 71.1–4.9) of complexes **1** (A) and **2** (B) in CDCl_3 at 298 K.**Figure 5.** Phase-sensitive NOESY spectrum of complex **1** (range δ_{H} 4.13–2.41) in CDCl_3 at 298 K. Only positive levels are plotted.

mobility. However, no interconversion of the two isomers or decomposition of any kind was noted.

Assignment of ^1H and ^{13}C spectra was based on COSY, HETCOR, and NOESY spectra as has been previously reported from our laboratory on technetium complexes.^{2bc,9} Differentiation of *endo* from *exo* protons was based on NOE correlation peaks. Specifically, in the case of the *syn* isomer, NOE correlation peaks are expected between the protons on the side chain on nitrogen and the *endo* protons of the chelated backbone (Figure 5), while in the case of the *anti* isomer they are expected between the side chain and the *exo* protons (Figure 6).

As can be seen from Table 2, the *syn* isomer follows the trend consistently reported in the literature,^{2bc,6cef,9,10} according to which the *endo* protons appear downfield compared to the *exo* ones. The difference in chemical shifts between the *exo* and *endo* protons is 0.6–0.7 ppm and is commonly attributed to

- (9) Papadopoulos, M. S.; Pelecanou, M.; Pirmettis, I. C.; Spyriounis, D.; Raptopoulou, C. P.; Terzis, A.; Stassinopoulou, C. I.; Chiotellis, E. *Inorg. Chem.* **1996**, *35*, 4478.
- (10) (a) John, C. S.; Francesconi, L. C.; Kung, H. F.; Wehri, S.; Graczyk, G.; Carroll, P. *Polyhedron* **1992**, *11*, 1145. (b) Rao, T. N.; Brixner, D. I.; Srinivasan, A.; Kasina, S.; Vanderheyden, J.-L.; Wester, D. W.; Fritzberg, A. R. *Appl. Radiat. Isotop.* **1991**, *42*, 525.

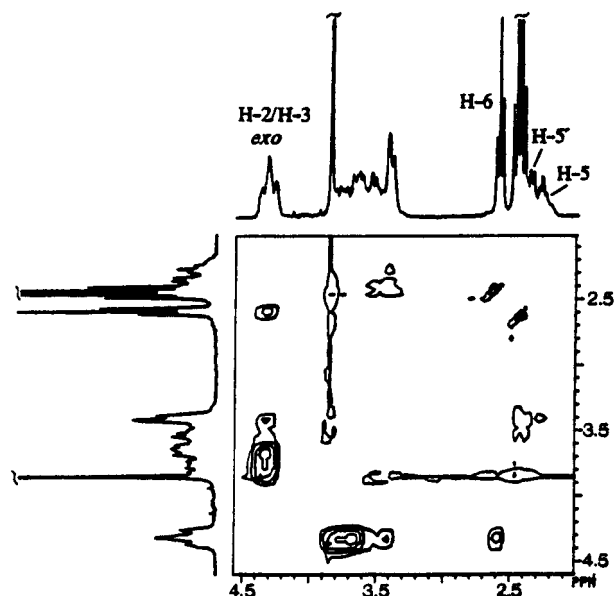


Figure 6. Phase-sensitive NOESY spectrum of complex **2** (range δ_H 4.54–2.98) in $CDCl_3$ at 298 K. Only positive levels are plotted.

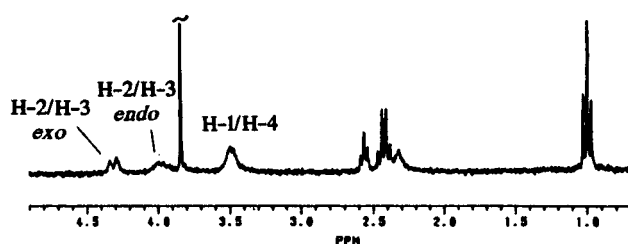


Figure 7. 1H NMR spectrum of the $Tc=O$ analogue of complex **2** (range δ_H 4.90–0.72) in $CDCl_3$ at 298 K.

the anisotropic effects of the $Re=O$ and $Tc=O$ core.^{6c,e,f,10} The situation is very different with the *anti* isomer **2**. First of all, the decreased mobility of the chelated backbone makes the geminal protons on C5 diastereotopic, appearing as two multiplets at δ_H 2.35 and 2.25. On the average, they are shifted upfield by 1.62 ppm compared to the corresponding protons of the *syn* isomer. Carbon C5 also appears shifted upfield by 10.7 ppm compared to the corresponding carbon of the *syn* isomer (Figure 4). Since carbon C5 and its protons are now at the *exo* face of the molecule, the upfield shift is consistent with that usually observed. Most important is the fact that this trend is not followed by protons C1, C2, C3, and C4 of the chelated backbone. The presence of NOE correlation peaks between the multiplet at δ_H 2.57 belonging to protons on C6 and the most downfield multiplets at δ_H 4.33 and 4.30 (Figure 6) indicates that these peaks belong to the H2/H3 *exo* protons. Another interesting point is that *exo* and *endo* protons on C1 have the same chemical shift despite their different orientations with respect to the $Re=O$ core (Table 2). The $Tc=O$ analogue^{2f} of complex **2** displays analogous behavior (Figure 7): the H2/H3 *exo* protons appear at δ_H 4.3, the H2/H3 *endo* protons are at δ_H 4.0, and the H1/H4 *endo* and *exo* protons are lumped together at δ_H 3.5.

These data on the *anti* isomers are the first example in the literature of NMR studies of oxorhenium and oxotechnetium complexes in which *exo* protons of the chelated backbone do not appear upfield compared to their *endo* geminals. Therefore, we are forced to reconsider the role of the oxorhenium and oxotechnetium cores as the sole cause of the observed magnetic anisotropy. Other mechanisms such as the chemical bond anisotropies of the side chain or the effect of the lone pairs on

coordinated sulfur may also be operating. According to this hypothesis, the different arrangement of the tridentate ligand about the $Re=O$ or $Tc=O$ core in the *syn* and *anti* isomers would modify the relative contributions of each mechanism and would account for the differences observed between the *syn* and *anti* isomers.

It is noted that 1H and ^{13}C chemical shifts do not change significantly on going from oxorhenium to oxotechnetium,^{2b,f} indicating structural similarity between $Re=O$ and $Tc=O$ analogues. Differences are observed, however, in the mobility of the chelated backbone, with $Re=O$ analogues being less flexible than $Tc=O$. For comparison purposes, the ΔG^\ddagger for conformational inversion of the *syn* complex of $Tc=O$ in $CDCl_3$ was calculated by the same method as mentioned earlier and was found to be 12.0 kcal/mol compared to the 13.9 kcal/mol of the $Re=O$ analogue. As a result, the chelated moieties S1–C1–C2–N and S2–C4–C3–N of the $Tc=O$ *syn* complex give identical proton and carbon spectra at 298 K due to motional averaging of the different conformations on the NMR time scale,^{2b} in contrast to the $Re=O$ complex, which, at the same temperature, is in slow exchange.

Conclusions. The simultaneous action of the tridentate *N,N*-bis-(2-mercaptoethyl)-*N',N'*-diethylethylenediamine and the monodentate 4-methoxythiophenol on a suitable $Re(O)$ precursor results in the formation of two isomers (*syn* and *anti*) due to the different orientation of the N substituent with respect to the $Re=O$. The *syn* isomer is preferably formed, while the *anti* isomer forms in small amounts. X-ray crystallography and NMR data show that the complexes have the same structure in the solid phase and in solution. Under the conditions employed during synthesis and spectral studies, no interconversion of the two isomers was noted. The *syn* isomer has a trigonal bipyramidal geometry, whereas the square pyramidal geometry is adopted by the *anti* isomer. NMR studies demonstrated that the direction of the side chain greatly influences the appearance of the spectra and the fluxional mobility of the SNS backbone. The isomeric set was also formed in high yield at the tracer level using ^{186}Re –citrate as precursor. The identity of ^{186}Re complexes was determined by comparative HPLC studies with authentic reference samples at the carrier level. This study provides information on the [SNS][S] mixed-ligand system, which should be useful in the preparation and characterization of biologically significant molecules labeled with $^{186/188}Re$.

Experimental Section

Materials and Methods. *Caution!!!* Rhenium-186 is a β - and γ -emitter and special precautions should be taken. IR spectra were recorded as KBr pellets in the range 4000–500 cm^{-1} on a Perkin-Elmer 1600 FT-IR spectrophotometer and were referenced to polystyrene. The NMR spectra were recorded in deuteriochloroform on a Bruker AC 250E spectrometer. Elemental analyses were performed on a Perkin-Elmer 2400/II automatic analyzer. High-performance liquid chromatography (HPLC) analysis was performed on a Waters chromatograph equipped with a 600E delivery system and a μ -Bondapak C-18 column using 85% methanol as the mobile phase at a 1.0 mL/min flow rate. Rhenium complexes were detected by a photodiode array detector (Waters 991 PDA) recording the UV–vis spectrum of the eluting complexes and a Beckman 171 radioisotope detector.

All laboratory chemicals were reagent grade. The 4-methoxythiophenol used as coligand was purchased from Fluka. The tridentate ligand was synthesized by reaction of the *N,N*-dimethylethylenediamine with ethylene sulfide in an autoclave at 110 $^\circ C$ as described previously, and the compound was purified by vacuum distillation.¹¹ $ReOCl_3 \cdot (PPh_3)_2$ was prepared according to the literature,¹² while precursors ReO –

(11) Corbin, J. L.; Miller, K. F.; Pariyadath, N.; Wherland, S.; Bruce, L. A.; Stiefel, E. I. *Inorg. Chim. Acta.* **1984**, *90*, 41.

(12) Chatt, J.; Rowe, G. A. *J. Chem. Soc.* **1962**, 4019.

(eg)₂ and Re(O)–citrate were generated *in situ* by known methods¹³ as described in detail in the following.

Synthesis of ReO[(C₂H₅)₂NCH₂CH₂N(CH₂CH₂S)]₂[SC₆H₄OCH₃]₂ from [ReO(eg)₂]⁺, Method A. The rhenium glycolate anion, [ReO(eg)₂][−], was prepared from 125 mg (0.2 mmol) of Bu₄NReOCl₄¹⁴ and 1.0 mL of ethylene glycol in 15 mL of EtOH *in situ*. To this solution were added 45 mg (0.2 mmol) of *N,N*-bis(2-mercaptoethyl)-*N,N'*-diethylethylenediamine (L1H₂) and 28 mg (0.2 mmol) of 4-methoxythiophenol (L2H) in 1.0 mL of dichloromethane and stirred at room temperature for 30 min. A green solid immediately precipitated from the reaction mixture. Volatiles were carefully removed under reduced pressure. The pH of the residue was adjusted to 9 with 0.5 N NaOH and the mixture was extracted two times with dichloromethane. Analysis of the solution by HPLC (C-18 RP column using 85/15 methanol/water as the mobile phase and 1 mL/min flow rate) demonstrated the formation of two complexes in a ratio of 25/1. The combined organic extracts were dried over MgSO₄, the volume was reduced to 5 mL by rotary evaporation at room temperature, and 5 mL of MeOH was added. Slow evaporation of the solvents at room temperature afforded the major product of the reaction as a green solid (**1**, *syn* isomer, 50% yield). The minor complex was separated as an orange solid from the filtrate upon standing at −20 °C for several days (**2**, *anti* isomer, 2% yield). Crystals suitable for X-ray crystallography were obtained by recrystallization from EtOH/CH₂Cl₂ for both products.

1 (*syn*): *R*_f = 0.40 (silica gel, 2/1/1 benzene/CH₂Cl₂/CH₃OH); FT-IR (cm^{−1}, KBr pellet) 946 (Re=O). Anal. Calcd for C₁₇H₂₉N₂O₂S₃Re: C, 35.46; H, 5.08; N, 4.87; S, 16.70. Found: C, 35.35; H, 4.76; N, 4.54; S, 16.32.

2 (*anti*): *R*_f = 0.45 (silica gel, 2/1/1 benzene/CH₂Cl₂/CH₃OH); FT-IR (cm^{−1}, KBr pellet) 963 (Re=O). Anal. Calcd for C₁₇H₂₉N₂O₂S₃Re: C, 35.46; H, 5.08; N, 4.87; S, 16.70. Found: C, 35.20; H, 5.00; N, 4.96; S, 16.88.

Synthesis from ReOCl₃(PPh₃)₂, Method B. To a stirred suspension of trichlorobis(triphenylphosphine)rhenium(V) oxide (166 mg, 0.2 mmol) in methanol (10 mL) was added 1 N CH₃COONa in methanol (2 mL, 2 mmol). A mixture of *N,N*-bis(2-mercaptoethyl)-*N,N'*-diethylethylenediamine (L1H₂) (45 mg, 0.2 mmol) and 28 mg (0.2 mmol) of 4-methoxythiophenol (L₂H) was added under stirring. The solution was refluxed until the green-yellow color of the precursor turned to dark green. After being cooled to room temperature, the reaction mixture was diluted with CH₂Cl₂ (30 mL) and then washed with water. The organic layer was separated from the mixture and dried over MgSO₄. The volume of the solution was reduced to 5 mL and then 5 mL of methanol was added. Analysis of the solution by HPLC (C-18 RP column using 85/15 methanol/water as the mobile phase and a flow rate of 1 mL/min) demonstrated the formation of two complexes in a ratio of 25/1. Only the major product was isolated as a green solid. Yield: 45%.

Synthesis from ReO–citrate, Method C. To a solution of SnCl₂ (38.9 mg, 0.2 mmol) in 0.5 M citric acid (5 mL) was added 57.8 mg (0.2 mmol) of KReO₄. To this mixture were added 45 mg (0.2 mmol) of L1H₂ and 28 mg (0.2 mmol) of L2H in 1 mL of dichloromethane dropwise and stirred at room temperature for 30 min. The pH was adjusted to 9 with 0.5 N NaOH and the mixture was extracted with CH₂Cl₂. Analysis of the organic phase by HPLC (C-18 RP column eluted by 85/15 methanol/water at a flow rate of 1 mL/min) demonstrated the formation of only one complex. Green crystals were isolated by a procedure similar to that described earlier. Yield: 30%. IR (KBr): 945 cm^{−1} (Re=O).

Synthesis at Tracer ¹⁸⁶Re Level. ¹⁸⁶ReO₄[−] (2 mCi, 1 mL) was added to a solution of 1 mL of 0.5 M of citric acid containing 1 mg of SnCl₂. This solution was transferred in a centrifuge tube containing equimolar quantities (0.02 mmol) of L1H₂ and L2H. The mixture was agitated in a vortex mixer and left to react at room temperature for 10 min. The pH of the reaction mixture was adjusted to 9 with 0.5 N NaOH and the aqueous phase was extracted with two successive 1.5

Table 4. Summary of Crystal, Intensity Collection, and Refinement Data

	1	2
formula	C ₁₇ H ₂₉ N ₂ O ₂ S ₃ Re	C ₁₇ H ₂₉ N ₂ O ₂ S ₃ Re
FW	575.80	575.80
<i>a</i> (Å)	14.109(4)	9.3850(7)
<i>b</i> (Å)	7.518(2)	27.979(2)
<i>c</i> (Å)	20.900(5)	8.3648(6)
β (deg)	103.07(1)	99.86(1)
<i>V</i> (Å ³)	2159.4(9)	2163.9(3)
<i>Z</i>	4	4
<i>D</i> _{calcd} / <i>D</i> _{measd} (Mg m ^{−3})	1.771/1.75	1.767/1.75
space group	<i>P</i> 2 ₁ / <i>n</i>	<i>P</i> 2 ₁ / <i>n</i>
temp (K)	298	298
abs coeff (μ, mm ^{−1})	5.930	5.918
wavelength	Mo Kα, 0.71073	Mo Kα, 0.7107
max abs correction mode	1.81	1.64
reflections collected/unique	4130/4009	4062/3795
data used/parameters	3996/283	3747/241
goodness-of-fit on <i>F</i> ²	1.069	1.141
<i>R</i> indices ^a	<i>R</i> ₁ = 0.0661, <i>wR</i> ₂ = 0.1742 ^b	<i>R</i> ₁ = 0.0528, <i>wR</i> ₂ = 0.1349 ^b

^a *I* > 2σ(*I*), 3599 reflections for **1**, 2815 reflections for **2**; *R*₁ based on *F*², *wR*₂ based on *F*². ^b *R*₁ = Σ||*F*_o − |*F*_c||/Σ|*F*_o|; *wR*₂ = (Σ[w(*F*_o² − *F*_c²)²]/Σ[w(*F*_o²)²])^{1/2}.

mL portions of CH₂Cl₂. The combined organic extracts were dried over MgSO₄ and filtered. Analysis of the mixture performed by reversed-phase HPLC 85/15 methanol/water, flow rate 1 mL/min) showed a major radioactive peak (>95%) with a retention time of 8 min, while a second radioactive peak (<3%) was detected at 5.5 min. The identity of ¹⁸⁶Re complexes was determined by comparative HPLC studies, using as reference samples the complexes isolated at the carrier level.

X-ray Crystal Structure Determination. A green crystal of the *syn* isomer, **1**, with dimensions 0.10 × 0.50 × 0.50 mm was mounted in air, and diffraction measurements were made on a Crystal Logic Dual Goniometer diffractometer using graphite monochromated Mo radiation. An orange crystal of the *anti* isomer, **2**, (0.08 × 0.40 × 0.50 mm), was mounted in air, and data collection was performed on a P2₁ Nicolet diffractometer upgraded by Crystal Logic using Zr-filtered Mo radiation. Unit cell dimensions were determined and refined by using the angular settings of 25 automatically centered reflections in the range 11 < 2θ < 23 and they appear in Table 4. Intensity data were recorded using a θ–2θ scan. Three standard reflections monitored every 97 reflections showed less than 3% variation and no decay. Lorentz, polarization, and ψ-scan absorption corrections were applied using Crystal Logic software. The structures were solved by direct methods using SHELXS-86 and refined by full-matrix least-squares techniques on *F*² with SHELXL-93.¹⁵

1: 2θ(max) = 51°; scan speed = 3.5°/min; scan range = 2.5 plus *a*₁*a*₂ separation; data collected/unique/used, 4130/4009 (*R*_{int} = 0.0122)/3996; 283 parameters refined; for all data *R*₁/*wR*₂/GOF, 0.0757/0.1901/1.110; [Δσ]_{max} = 0.100; [Δρ]_{max}/[Δρ]_{min} = 2.868/2.720 e/Å³ in the vicinity of the heavy metal; the hydrogen atoms of the methyl groups, the phenyl group, and the methylene corresponding to C1 and C3 were introduced at calculated positions as riding on bonded atoms; the rest were located by difference maps and are refined isotropically.

2: 2θ(max) = 50°; scan speed = 3.0°/min; scan range = 2.5 plus *a*₁*a*₂ separation; data collected/unique/used, 4062/3795 (*R*_{int} = 0.0330)/3747; 241 parameters refined; for all data *R*₁/*wR*₂/GOF, 0.0888/0.2798/1.785; [Δσ]_{max} = 0.004; [Δρ]_{max}/[Δρ]_{min} = 3.050/−2.449 e/Å³ in the vicinity of the heavy metal; all hydrogen atoms were introduced at calculated positions as riding on bonded atoms and their positions were refined isotropically.

(13) (a) Morgan, G. F.; Deblaton, M.; Hussein, W.; Thornback, J. R.; Evrard, G.; Durant, F.; Stach, J.; Abram, U.; Abram S. *Inorg. Chim. Acta* **1991**, *190*, 257. (b) Rao, T. N.; Adhikesavala, D.; Cameran, A.; Fritzberg, A. R. *Inorg. Chim. Acta* **1991**, *180*, 63.
(14) Lis, T.; Jezowska-Trzebiatowska, B. *Acta Crystallogr., Sec. B*, **1976**, *33*, 1248.

(15) (a) Sheldrick, G. M. *SHELXS-86, Structure solving Program*; University of Göttingen: Göttingen, Germany, 1986. (b) Sheldrick, G. M. *SHELXL-93, Program of Crystal Structure Refinement*; University of Göttingen, Göttingen: Germany, 1993. (c) Atomic scattering factors were taken from *International Tables for X-ray Crystallography*; Kynoch Press: Birmingham, 1974; Vol. IV.

All non-hydrogen atoms were refined anisotropically in both structures. No extinction corrections were applied. Selected bond distances and angles are given in Table 1.

NMR Studies. The ^1H (250.13 MHz) and ^{13}C (62.90 MHz) NMR spectra were recorded on a Bruker AC 250E spectrometer equipped with an Aspect 3000 computer (using the DISNMR program, version 1991) and a 5 mm $^{13}\text{C}/^1\text{H}$ dual probe head (^1H 90° pulse width = 10.2 μs , ^{13}C 90° pulse width = 10.4 μs). Samples were dissolved in CDCl_3 at a concentration of ca. 1–2%. High-temperature studies were performed in toluene- d_8 . Except for the variable-temperature studies, spectra were obtained at 298 K (25 °C). Chemical shifts (δ) are relative to internal TMS.

2D ^1H – ^1H shift correlated spectra (COSY) were acquired with a spectral window of 2180 Hz, 1024 data points, 128 t_1 increments, and 1 s relaxation delay between pulse cycles. The data were processed by applying a sine-bell (nonshifted) multiplication in both dimensions and by zero-filling to 512 data points in the F_1 domain. After inspection the final matrix (digital resolution 4.3 Hz/point) was symmetrized.

Phase-sensitive NOESY spectra were acquired with a spectral window of 2180 Hz, 512 data points, 128 t_1 increments, a mixing time of 1 s, and a 1 s relaxation delay between cycles. The data were processed by applying a sine-bell squared ($\pi/2$ shifted) multiplication in both dimensions and by zero-filling to 512 data points in the F_1 dimension. After inspection the final matrix was symmetrized.

2D ^{13}C – ^1H shift-correlated spectra (HETCOR) were obtained with spectral windows of 2180 Hz in the F_1 dimension and 8930 Hz in the

F_2 dimension, 2048 data points, 128 t_1 increments, and relaxation delay of 1 s. The experiment was optimized for $J(^{13}\text{C},^1\text{H}) = 130$ Hz. The data were processed by applying a sine-bell ($\pi/2$ shifted) multiplication in both dimensions and by zero-filling to 256 data points in the F_1 dimension. Digital resolution was 17.0 Hz/point in the F_1 dimension and 8.7 Hz/point in the F_2 dimension.

Calculation of ΔG^\ddagger . For the variable-temperature studies, the coalescence region for every pair of ^{13}C resonances under investigation was initially determined by obtaining spectra at 5° intervals. Spectra were then obtained in the coalescence region at 0.5° intervals to determine the coalescence temperature T_c . Complex 1: T_c is 284.0 K for C2/C3 ($\Delta\nu$ in the absence of exchange = 95.4 Hz) and 280.0 K for C1/C4 ($\Delta\nu$ in the absence of exchange = 43.8 Hz). Complex 2: T_c is 313.0 K for C2/C3 ($\Delta\nu = 24.2$ Hz) and 315.0 K for C1/C4 ($\Delta\nu = 34.5$ Hz).

Acknowledgment. A.T. is grateful to Mrs. A. Athanasiou for financial support.

Supporting Information Available: Tables of crystal data, fractional atomic coordinates and anisotropic thermal parameters for all non-hydrogen atoms, fractional atomic coordinates of H-atoms, and full bond lengths and angles (11 pages). Ordering information is given on any current masthead page.

IC9604167